THE FUNGUS *TRICHOPHYTON REDELLII* SP. NOV. CAUSES SKIN INFECTIONS THAT RESEMBLE WHITE-NOSE SYNDROME OF HIBERNATING BATS

Jeffrey M. Lorch,[1] **Andrew M. Minnis,**[2] **Carol U. Meteyer,**[3,5] **Jennifer A. Redell,**[4] **J. Paul White,**[4] **Heather M. Kaarakka,**[4] **Laura K. Muller,**[3] **Daniel L. Lindner,**[2] **Michelle L. Verant,**[1] **Valerie Shearn-Bochsler,**[3] **and David S. Blehert**[3,6]

[1] Department of Pathobiological Sciences, School of Veterinary Medicine, University of Wisconsin-Madison, 1656 Linden Drive, Madison, Wisconsin 53706, USA

[2] United States Forest Service, Northern Research Station, Center for Forest Mycology Research, One Gifford Pinchot Drive, Madison, Wisconsin 53726, USA

[3] United States Geological Survey, National Wildlife Health Center, 6006 Schroeder Road, Madison, Wisconsin 53711, USA

[4] Bureau of Natural Heritage Conservation, Wisconsin Department of Natural Resources, 101 S Webster Street, Madison, Wisconsin 53707, USA

[5] Current address: United States Geological Survey National Center, Environmental Health, 12201 Sunrise Valley Drive, Reston, Virginia 20192, USA

[6] Corresponding author (email: dblehert@usgs.gov)

ABSTRACT: Before the discovery of white-nose syndrome (WNS), a fungal disease caused by *Pseudogymnoascus destructans*, there were no reports of fungal skin infections in bats during hibernation. In 2011, bats with grossly visible fungal skin infections similar in appearance to WNS were reported from multiple sites in Wisconsin, US, a state outside the known range of *P. destructans* and WNS at that time. Tape impressions or swab samples were collected from affected areas of skin from bats with these fungal infections in 2012 and analyzed by microscopy, culture, or direct DNA amplification and sequencing of the fungal internal transcribed spacer region (ITS). A psychrophilic species of *Trichophyton* was isolated in culture, detected by direct DNA amplification and sequencing, and observed on tape impressions. Deoxyribonucleic acid indicative of the same fungus was also detected on three of five bat carcasses collected in 2011 and 2012 from Wisconsin, Indiana, and Texas, US. Superficial fungal skin infections caused by *Trichophyton* sp. were observed in histopathology for all three bats. Sequencing of the ITS of *Trichophyton* sp., along with its inability to grow at 25 C, indicated that it represented a previously unknown species, described herein as *Trichophyton redellii* sp. nov. Genetic diversity present within *T. redellii* suggests it is native to North America but that it had been overlooked before enhanced efforts to study fungi associated with bats in response to the emergence of WNS.

Key words: Bat, dermatophyte, fungal infection, hibernation, *Trichophyton*, white-nose syndrome.

INTRODUCTION

Dermatophytes (defined here on the basis of taxonomy) are common on many groups of free-ranging mammals (Mantovani et al. 1982). Although dermatophytes have been observed on hibernating bats (Courtin et al. 2010; Vanderwolf et al. 2013b), they have not been linked to disease. Indeed, we are unaware of reports of fungal skin infections in hibernating bats in North America before the arrival of white-nose syndrome (WNS), a deadly disease caused by the fungus *Pseudogymnoascus destructans* (Blehert et al. 2009; Lorch et al. 2011). While it is possible that bats are generally resistant to fungal infections during hibernation (with the exception of *P. destructans*), it seems more plausible that nonlethal fungal infections have gone undetected. Learning more about these fungi and how bats cope with them could provide insight into why WNS is deadly to many North American bats.

Beginning in winter 2011, the Wisconsin (US) Department of Natural Resources (WDNR) reported hibernating bats with grossly visible white fungus similar to some of the clinical signs that characterize WNS (Fig. 1A). However, Wisconsin was outside the known range of WNS at that time (US Fish and Wildlife Service 2014). Potentially infected animals were submitted to the US Geological Survey–National Wildlife
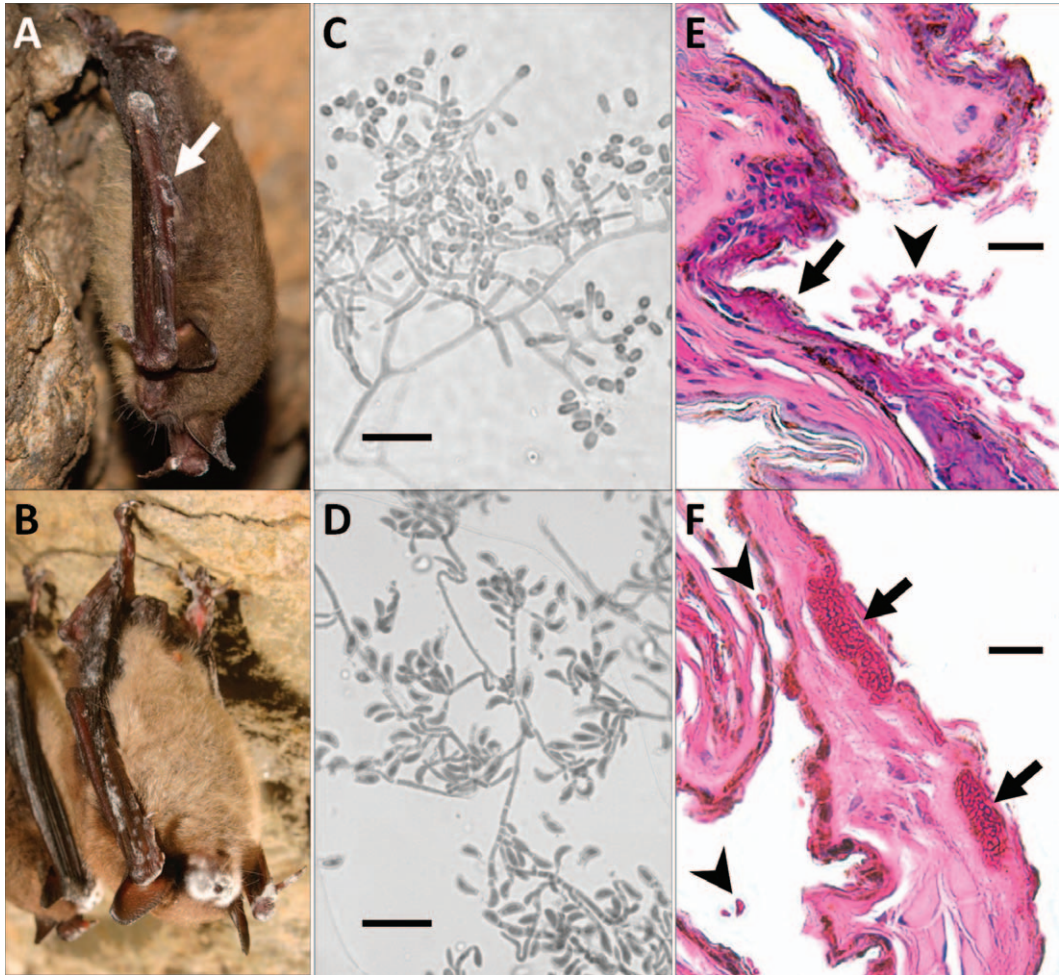
FIGURE 1. Comparison between *Trichophyton redellii* infection (top panels) and *Pseudogymnoascus destructans* infection (i.e., white-nose syndrome [WNS]; bottom panels) in bats. Bats infected with *T. redellii* have visible white fungal growth on the ears, legs, wings, tail, or uropatagium (A); lesions may manifest as a distinct ring (arrow); the muzzle often lacks clinical signs of infection. Bats with WNS generally have visible fungus on the muzzle in addition to other areas of unfurred skin (B). Fungal tape impressions collected from bats with clinical signs of *T. redellii* infection display radially symmetric obovate to pyriform microconidia (C), as opposed to the asymmetrical curved conidia typical of *P. destructans* (D). In histologic sections (prepared with periodic acid–Schiff staining), the wing skin of bats with *T. redellii* infections (E) generally have superficial colonization and invasion of the keratin layers by the dermatophyte (arrow); aerial hyphae and fertile structures in the form of conidiophores and microconidia may also be present (arrowhead). In contrast, histologic cross sections of wing skin from bats with WNS (F) typically display cup-like aggregations of fungal hyphae (arrows), erosion of the epidermis, and occasional curved conidia (arrowheads). Scale bars=20 μm.

Health Center (NWHC; Madison, Wisconsin, USA) for diagnostic testing and were shown to be negative for WNS by histopathology and negative for *P. destructans*. We describe the cause of these skin infections and provide information on how to distinguish them from WNS.

MATERIALS AND METHODS

Sample collection

In winter 2011 and 2012, NWHC received bats that had visible fungal skin infections in the field but subsequently were found negative for WNS by histopathology and negative for *P. destructans* by PCR (Muller et al. 2013)

TABLE 1.   Bats sampled to characterize fungi that cause skin infections unrelated to white-nose syndrome. Identifiers represent US Geological Survey–National Wildlife Health Center case and accession numbers of whole bat carcasses, swabs, and fungal tape impressions submitted for testing. Clinical signs refer to the presence (+) or absence (−) of visible fungus on the skin when the bats were observed in the field. Analyses performed included culture (C) from swabs, direct amplification and sequencing of a portion of the fungal internal transcribed spacer region (DAS) from swabs and carcass wing tissue, microscopic examination (M) of fungal tape impressions collected directly from bat skin, and histopathologic examination (H) of wing tissue.

Identifier	*Myotis* host species	Collection location[a]	Clinical signs	Sample type	Analyses performed
23489-01	*lucifugus*	Greene Co., Indiana, USA	+	Carcass	DAS, H
23493-01	*lucifugus*	Pierce Co., Wisconsin, USA	+	Carcass	DAS, H
23863-01	*velifer*	Wheeler Co., Texas, USA	+	Carcass	DAS, H
23863-02	*velifer*	Wheeler Co., Texas, USA	+	Carcass	DAS, H
23863-03	*velifer*	Wheeler Co., Texas, USA	+	Carcass	DAS, H
44738-01	*lucifugus*	Grant Co., Wisconsin, USA	+	Swab	C, DAS
44738-02	*lucifugus*	Grant Co., Wisconsin, USA	+	Swab, tape impression	C, DAS, M
44738-03	*lucifugus*	Grant Co., Wisconsin, USA	+	Swab, tape impression	C, DAS, M
44738-04	*lucifugus*	Grant Co., Wisconsin, USA	+	Swab	C, DAS
44738-05	*lucifugus*	Grant Co., Wisconsin, USA	+	Swab	C, DAS
44738-06	*lucifugus*	Grant Co., Wisconsin, USA	+	Swab	C, DAS
44738-07	*lucifugus*	Pierce Co., Wisconsin, USA	+	Swab	C, DAS
44738-08	*lucifugus*	Pierce Co., Wisconsin, USA	+	Swab	C, DAS
44738-09	*lucifugus*	Pierce Co., Wisconsin, USA	+	Swab, tape impression	C, DAS, M
44738-10	*lucifugus*	Pierce Co., Wisconsin, USA	+	Swab	C, DAS
44738-11	*lucifugus*	Pierce Co., Wisconsin, USA	−	Swab	C, DAS
44738-12	*lucifugus*	Pierce Co., Wisconsin, USA	−	Swab	C, DAS

[a] Co. = county.

and culture analyses. These included a little brown bat (*Myotis lucifugus*) from Wisconsin; a little brown bat from Indiana, US; and three cave bats (*Myotis velifer*) from Texas, US (Table 1). The bats were euthanized by personnel of the WDNR, Indiana Department of Natural Resources, and Texas Parks and Wildlife Department in accordance with applicable state laws.

Nonlethal samples were collected from two sites in Wisconsin in March 2012 (WDNR's Animal Care and Use Committee Protocol 11-RedellD-01). PurFlock® sterile nylon flocked swabs (Puritan Medical Products Company LLC, Guilford, Maine, USA) moistened with 15 µL sterile phosphate-buffered saline were wiped against the wing skin of hibernating bats with white fungal growth and stored in sterile 1.5-mL microcentrifuge tubes (*n*=10). The forearms of animals without visible fungal growth were also swabbed to serve as controls (*n*=2). Chilled swab samples were transported to NWHC for processing within 24 h of collection. Fungal tape impressions (Fungi-Tape™, Scientific Device Laboratory, Des Plaines, Illinois, USA) were also taken from three of the bats that were swabbed. The area of the tape that contacted the skin was circled with a marker, the tape was affixed to a microscope slide, and the encircled area was examined using a microscope (400× magnification).

Assessment of fungi on infected bat skin

Swab samples were subjected to culture analysis by streaking the swabs onto Sabouraud dextrose agar plates with chloramphenicol and gentamicin (SDA; BD Diagnostic Systems, Sparks, Maryland, USA) as described by Lorch et al. (2010). The culture plates were incubated at 7 C and checked once per week for 8 wk. Fungi isolated from initial plates were thereafter maintained on SDA. To identify fungal isolates, we sequenced the internal transcribed spacer region (ITS). A sterile toothpick was used to scrape mycelia from pure cultures on fungal growth media. The scraped material was transferred to 0.2-mL strip tubes containing 20 µL microLYSIS® solution (Gel Company, San Francisco, California, USA), and the cells were lysed according to the manufacturer's instructions. Polymerase chain reaction targeting ITS was performed using universal fungal primers ITS1-F and ITS4 (Gardes and Bruns 1993; cycling conditions: 94 C for 3 min followed by 40 cycles of 94 C for 1 min, 53 C for 1 min, and 72 C for 3 min, with a final extension for

10 min at 72 C). All PCR reactions were conducted using GoTaq® Flexi DNA polymerase (Promega Corporation, Madison, Wisconsin, USA) according to the manufacturer's instructions, with 0.5-µL template per 25-µL reaction. Additional loci of two fungal isolates of the bat-infecting fungus were sequenced: nuclear large subunit rRNA gene (LSU), DNA replication licensing factor MCM7 (*MCM7*), RNA polymerase II second largest subunit (*RPB2*), and translation elongation factor EF-1α (*TEF1*) as described by Minnis and Lindner (2013). The intergenic spacer region (IGS) was sequenced following the methods of Lorch et al. (2013), except that products were sequenced from both 5′- (using primer CNL12 [Anderson and Stasovski 1992]; IGS-5′) and 3′- (using primer CNS1 [White et al. 1990]; IGS-3′) ends. All newly generated sequences were deposited into GenBank.

After swabs were streaked on fungal growth medium, each swab was returned to its original collection tube, and 50 µL of micro-LYSIS solution was added. The swab was swirled in the solution for 30 s and allowed to soak for an additional 5 min. Fungal cells in the solution were lysed following the manufacturer's instructions. For whole carcasses submitted for diagnostic testing, a small piece of wing tissue was excised, and DNA was extracted as described by Lorch et al. (2010). Polymerase chain reaction and double-stranded sequencing of PCR products were performed using primers ITS1-F and ITS4 as described above. Histopathologic analyses were performed on wing skin from the bat carcasses submitted for diagnostic evaluation (*n*=5) following the methods of Meteyer et al. (2009).

Phylogenetic analysis

The ITS sequences of isolates most commonly associated with the fungal infections were aligned with ITS sequences in GenBank (and newly generated sequences—see Results) of closely related fungi using the default settings of the online version (http://mafft.cbrc.jp/alignment/server/) of MAFFT v.7 (Katoh and Standley 2013). Rambaut's Se-AL v2.0a9 was used to adjust the resulting alignment, and areas with excessive gaps and ambiguously aligned regions were deleted. A maximum likelihood (ML) analysis was conducted with RAxML (Stamatakis 2006; Stamatakis et al. 2008) via RAxML-HPC2 v7.6.6 using the CIPRES Science Gateway (Miller et al. 2010). All parameters were defaulted, but best scoring ML tree and bootstrap (BS) analyses were made in a single run, with 1,000 BS iterations and GTRGAMMA selected for the bootstrapping phase and final tree. Parsimony-based BS analyses (Felsenstein 1985) with 1,000 BS replicates and maxtrees unlimited, 10 random taxon-addition sequences and 100 trees held at each step, and all other parameters at default were conducted with PAUP* (Swofford 2003) to address clade support using an additional method.

Characterization of fungal isolates

Representative isolates of taxa described as new herein were incubated at 25 C and 10 C on SDA plates in the dark. Plates were inoculated by transferring fungal material with an inoculating needle; all isolates were inoculated in triplicate. Measurements and observations of cultures were made each week for 4 wk. Terminology and sample reference codes in parentheses for colony coloration are from Kornerup and Wanscher (1978). Microscopic observations were made of material from cultures mounted in 3% KOH or Cotton Blue (Largent et al. 1997). At least 30 conidia of each culture were measured. Length-to-width ratios are given as Q. Representative living cultures of taxa described as new herein were deposited at the Center for Forest Mycology Research (CFMR) in Madison, Wisconsin, and the Centraalbureau voor Schimmelcultures (CBS) in the Netherlands.

RESULTS

Assessment of fungi on infected bat skin

Swab samples from five of 10 infected bats yielded pure, heavy growth of a single fungus in culture after 10–30 d of incubation; no microbial growth was observed from samples collected from the remaining five animals with clinical signs or from the two bats without clinical signs (Table 2). Colony characteristics and microscopic observations of all fungal isolates were similar and were morphologically consistent with *Trichophyton*. Attempts to re-culture skin samples from the five bat carcasses to specifically target *Trichophyton* were unsuccessful, possibly because of the fungus' inability to survive freezing (bat carcasses were stored frozen).

Sequenced PCR products from direct amplification of the fungal ITS of samples from three of five bat carcasses most closely matched several undescribed

TABLE 2.   Results of analyses conducted to investigate the cause of fungal skin infections in hibernating bats unrelated to white-nose syndrome. Culture results are based on DNA sequencing of the internal transcribed spacer region (ITS) of fungi cultured from a given sample. Molecular results are based on direct amplification and DNA sequencing of the ITS from DNA extracted from a given tissue/swab sample. Microscopy results are based on tape impressions of white fungal material observed on bats in the field; these tape impressions were subsequently examined in the laboratory under a microscope, and fungi present were identified on the basis of morphology. All GenBank accession numbers represent sequences generated from fungal isolates except in cases for which either culture analyses were not performed or there was no fungal growth on culture medium.

Identifier	Culture result[a]	Molecular result	Microscopy result[a]	ITS GenBank accession[a]
23489-01	N/A	*Trichophyton redellii*	N/A	KM091312
23493-01	N/A	*Trichophyton redellii*	N/A	KM091313
23863-01	N/A	Could not be interpreted[b]	N/A	N/A
23863-02	N/A	*Debaryomyces* sp.	N/A	KM091320
23863-03	N/A	*Trichophyton redellii*	N/A	KM091314
44738-01	*Trichophyton redellii*	*Trichophyton redellii*	N/A	KM091308
44738-02	No fungal growth	*Trichophyton redellii*	Consistent with *Trichophyton*	KM091315
44738-03	*Trichophyton redellii*	*Trichophyton redellii*	Consistent with *Trichophyton*	KM091307
44738-04	No fungal growth	*Trichophyton redellii*	N/A	KM091316
44738-05	*Trichophyton redellii*	*Trichophyton redellii*	N/A	KM091309
44738-06	*Trichophyton redellii*	*Trichophyton redellii*	N/A	KM091310
44738-07	No fungal growth	*Trichophyton redellii*	N/A	KM091317
44738-08	*Trichophyton redellii*	*Trichophyton redellii*	N/A	KM091311
44738-09	No fungal growth	*Trichophyton redellii*	Consistent with *Trichophyton*	KM091318
44738-10	No fungal growth	*Trichophyton redellii*	N/A	KM091319
44738-11	No fungal growth	No DNA amplification	N/A	N/A
44738-12	No fungal growth	No DNA amplification	N/A	N/A

[a] N/A = not applicable.

[b] Superimposed peaks in the DNA sequence data prevented interpretation of results.

Trichophyton/Arthroderma spp. isolated from cave soil (Lorch et al. 2013) and *Arthroderma quadrifidum* (Brasch and Gräser 2005) from the GenBank database. However, the ITS of *A. quadrifidum* demonstrated only 98% identity with that from the fungus detected on bats, indicating that the bat-infecting fungus likely represented a novel species. Three genetic variants of the fungus were detected on the three bats, differing from one another by one to four single nucleotide polymorphisms (SNPs) across the ITS. Sequencing results from direct PCR analysis from a fourth bat most closely matched *Debaryomyces* sp. (99% identity to *Debaryomyces marama*, GenBank accession JN942650), and that from the fifth animal was not readable because of superimposed peaks. The ITS of all fungal isolates obtained from the swab samples were identical to two of the ITS sequence variants of the putative *Trichophyton* species obtained by direct PCR and DNA sequence analysis of skin samples from bat carcasses described earlier. Fungal ITS was also amplified and sequenced directly from DNA extracted from swab samples, and all 10 swabs yielded amplicons that were identical to the ITS sequences of the fungi isolated in culture. No amplicons were produced from direct PCR amplification of the samples collected from bats without clinical signs of fungal infection. Tape impressions taken from three bats contained dense fungal microconidia and hyphae morphologically consistent with those observed in histopathology and in culture (Fig. 1C). The concordance of microscopic, culture, and molecular evidence (Table 2) suggest that a putative *Trichophyton* species was the cause of the skin infections observed in the hibernating bats.

Sequences representing IGS-5′, *MCM7*, *RPB2*, and *TEF1* of the bat fungus were in

agreement with the ITS data, most closely matching the few species of *Trichophyton/Arthroderma* (90–98% identity for IGS-5′, 82–85% identity for *MCM7*, 86–91% identity for *RPB2*, and 90–92% identity for *TEF1*) for which sequences of these loci were available in GenBank. The IGS-3′ sequence was more divergent, but portions of the sequence again most closely matched various species of *Trichophyton/Arthroderma*. Thus DNA sequence data from multiple loci supported the placement of the bat-infecting fungus within the dermatophyte group. The IGS-3′ sequence of the bat-infecting fungus demonstrated intraspecific variation at five SNPs over the 802-nucleotide region sequenced, and *MCM7* displayed similarly high identity (i.e., two SNPs over 591 nucleotides sequenced). However, IGS-5′, LSU, *RPB2,* and *TEF1* sequences were identical, indicating that the two variants likely represent a single species.

Fungal elements were observed in histopathology from all five bats examined. However, lesions diagnostic for WNS (Meteyer et al. 2009) and fertile structures characteristic of *P. destructans* (Fig. 1F; Gargas et al. 2009) were absent. Instead, fungi observed were associated with infections that were primarily superficial, with hyphae found on the surface of the skin, in the outer layers of keratin, and sometimes within intradermal pustules (Fig. 1E). Sessile, smooth-walled, obovate to pyriform microconidia borne laterally and terminally on hyphae were present in association with hyphal colonization and invasion of the keratin layer in three of the bats (cases 23489-01, 23863-01, 23863-03) and were suggestive of *Trichophyton* (Fig. 1E). Only vegetative hyphae lacking characteristics that allowed for morphologic identification were observed on the remaining two animals (cases 23493-01, 23863-02).

Phylogenetic analysis

Internal transcribed spacer DNA sequence data were used for the phylogenetic analysis because the other loci sequenced (i.e., IGS, LSU, *MCM7, RPB2, TEF1*) were poorly represented for *Trichophyton* and related fungi in GenBank (completing multigene phylogenetic analyses was not feasible with existing data). Our sampling of dermatophyte ITS sequences for this study followed that of Brasch and Gräser (2005). New DNA sequences were also generated from the original isolates used to describe *Trichophyton terrestre* (Durie and Frey 1957) and its purported teleomorph *A. quadrifidum* (Dawson and Gentles 1961) using cultures UAMH 657 and UAMH 2941 (from The University of Alberta Microfungus Collection and Herbarium), respectively, because these data were not previously available in GenBank (deposited for this study as GenBank accessions KM091305 and KM091306, respectively). Deoxyribonucleic acid amplification and sequencing for these isolates followed the methods described earlier.

The best tree generated from the ML analysis (Fig. 2) included a large, well-supported crown group consisting of the primarily anthropophilic and zoophilic species of dermatophytes (groups 1 and 2 as defined by Gräser et al. [2000]), and the remaining diversity included the primarily geophilic species of dermatophytes (group 3 species of Gräser et al. [2000]) as basal to the crown group. In general, the topology of the best tree was consistent with earlier studies (Gräser et al. 2000; Brasch and Gräser 2005), as was the generally poor resolution of relationships among many taxa. However, sequences that represented isolates of the dermatophyte recovered from bats in this study resided within the geophilic group and formed a well-supported clade (87% ML BS, 88% parsimony-based BS) recognized herein as *Trichophyton redellii* sp. nov. This clade is situated within another clade (86% ML BS, 96% parsimony-based BS) that includes *A. quadrifidum*, which shares only 98% identity with *T. redellii*. Divergence in the sequences of IGS-5′,
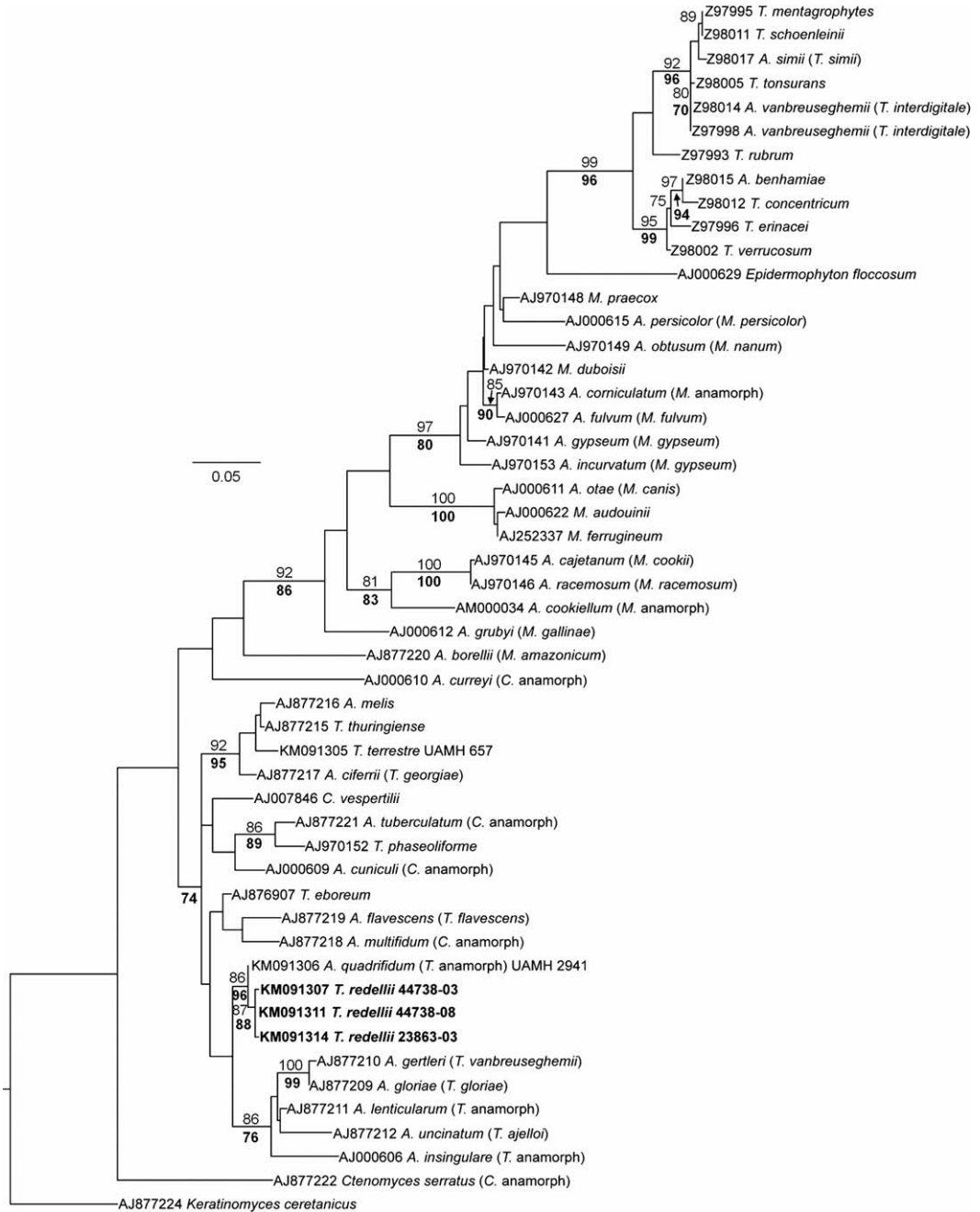
FIGURE 2.   Best tree resulting from the maximum likelihood analysis. Bootstrap support values ≥70% from 1,000 iterations from RAxML analysis are presented above branches, and bootstrap support values ≥70% from the 1,000 iterations from parsimony-based PAUP* analysis are bolded and presented below branches. Generic abbreviations are *A.* (*Arthroderma*), *C.* (*Chrysosporium*), *M.* (*Microsporum*), and *T.* (*Trichophyton*). GenBank accession numbers are followed by taxon name and, when appropriate, additional identifiers for each isolate. Scale bar=0.05 nucleotide substitutions per site.
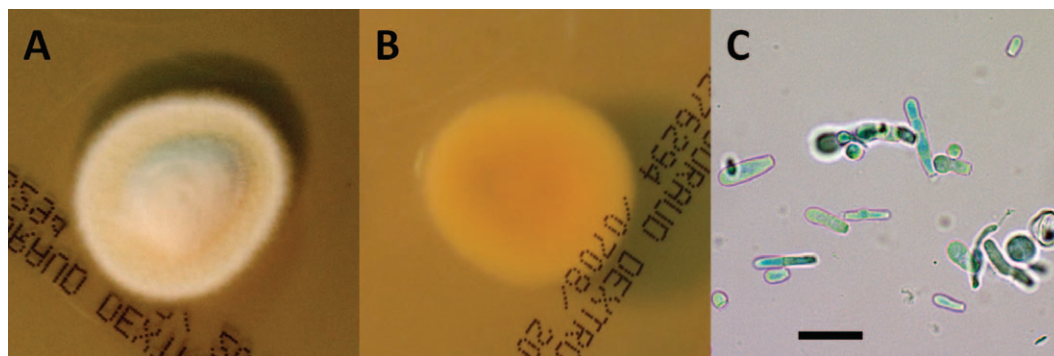
FIGURE 3. *Trichophyton redellii* (ex-type living culture): colony surface on Sabouraud dextrose agar (SDA) after 37 d incubated at 10 C in the dark (A); colony reverse on SDA after 37 d incubated at 10 C in the dark (B); conidia (C). Bar=20 μm.

IGS-3′, *MCM7*, *RPB2,* and *TEF1* of *A. quadrifidum* obtained as described earlier further supported that *T. redellii* is distinct from that species (IGS-5′: 87.1% identity among approximately 400 nucleotides aligned; IGS-3′: 85.8% identity among 489 nucleotides; *MCM7*: 93.7% identity among 552 nucleotides; *RPB2*: 97.2% identity among 861 nucleotides; *TEF1*: 98.3% identity among 850 nucleotides; *A. quadrifidum* [UAMH 2941]. GenBank accessions KM091301, KM091304, KM091288, KM091292, KM091296, respectively).

The ITS-based phylogenetic analysis also indicated that *T. terrestre* is not conspecific with its supposed teleomorph *A. quadrifidum* (Dawson and Gentles 1961; see Fig. 2). This was further supported by DNA sequence data from other loci showing significant divergence between the two isolates (*MCM7*: 86.6% identity among 552 nucleotides; *RPB2*: 92.0% identity among 861 nucleotides; *TEF1*: 95.1% identity among 850 nucleotides; *T. terrestre* [UAMH 657]. GenBank accessions KM091287, KM091291, KM091295, respectively).

Species Description

Trichophyton redellii: Minnis, J.M. Lorch, D.L. Lindner & Blehert, **sp. nov.** Fig. 3
MycoBank: MB809547

Diagnosis: This species is morphologically similar to *Trichophyton terrestre*, but differs in its lack of growth at 25 C and occurrence as an infectious agent on hibernating bats.

Holotype: US, Wisconsin, Grant Co., ex wing of hibernating *Myotis lucifugus*, 23 February 2012, collected by M. L. Verant, isolated by J. M. Lorch from NWHC No. 44738-03, dried culture on SDA (holotype, CFMR 44738-03H); ex-type living culture CBS 134551 = CFMR 44738-03; GenBank IGS (5′ end: KM091299; 3′ end: KM091302), ITS: KM091307, *MCM7*: KM091285, LSU: KM091297, *RPB2*: KM091289, *TEF1*: KM091293.

Etymology: The genitive species epithet honors the late David N. Redell for his discovery of the infections caused by this fungus and for his contributions to bat conservation and research.

Description: Colonies exhibited no growth on SDA after 30 d at 25 C, ca. 3–5.5 mm in diameter on SDA after 14 d at 10 C, 10.5–15.5 mm in diameter after 30 d at 10 C; somewhat mounded at center; surface white to near yellowish white (4A2), velutinous; margin uncolored becoming white, more or less even; reverse light yellow (3A5 or 4A5) to yellowish orange (4A7) near center and uncolored to

similarly colored as center to yellowish white (4A2) toward margin. Ascomata not observed. Aerial hyphae abundant, 2–6 μm in diameter, septate, hyaline, walls thin and smooth. Thallic conidia borne singly and laterally at right angles or terminally on aerial hyphae, sessile or on short, simple pedicels, with macroconidia, microconidia, and intermediate forms that make categorical distinction fairly inconsequential. Conidia 6–65 μm × 3–8 μm, length-to-width ratio (Q) = 1.2–13.8 (–21.7), ellipsoid, obpyriform, clavate, slightly apiosporous, cylindrical or irregular, 0–5-septate and constricted or not at septa, apices obtuse, bases slightly truncate with an annular frill, hyaline, walls thin and smooth. Chlamydospores forming in vegetative hyphae or individual cells of conidia in older cultures, more or less globose, hyaline, walls slightly thickened, up to approximately 22 μm in diameter.

Habitat and distribution: Found on hibernating *Myotis lucifugus* and *Myotis velifer*. Known from US: Indiana, Texas, Wisconsin.

Additional cultures examined: US, Wisconsin, Grant Co., ex wing of hibernating *Myotis lucifugus*, 23 February 2012, collected by M. L. Verant, isolated by J. M. Lorch from NWHC No. 44738-01, living culture CBS 134550 = CFMR 44738-01, GenBank ITS: KM091308; isolated by J. M. Lorch from NWHC No. 44738-05, living culture CBS 134552 = CFMR 44738-05, GenBank ITS: KM091309; isolated by J. M. Lorch from NWHC No. 44738-06, living culture CBS 134553 = CFMR 44738-06, GenBank ITS: KM091310; Pierce Co., ex wing of hibernating *Myotis lucifugus*, 19 March 2012, collected by M. L. Verant, isolated by J. M. Lorch from NWHC No. 44738-08; living culture CBS 134554 = CFMR 44738-08, GenBank IGS (5′ end: KM091300; 3′ end: KM091303), ITS: KM091311, *MCM7*: KM091286, LSU: KM091298, *RPB2*: KM091290, *TEF1*: KM091294.

DISCUSSION

The emergence of WNS highlighted our limited knowledge of fungi that colonize bat skin. Investigators have examined fungal communities found on hibernating bats (Johnson et al. 2013; Vanderwolf et al. 2013b) and in sediment of bat hibernacula (Lorch et al. 2013). However, fungi specialized for growth on mammalian skin were not prevalent in these studies. The most common fungus detected on bats with clinical infections in our study was the previously undescribed dermatophyte *Trichophyton redellii*. Geophilic species of *Trichophyton/Arthroderma* appear to be regular, although not necessarily abundant, inhabitants of caves and mines (Lorch et al. 2013; Vanderwolf et al. 2013a) and have occasionally been reported as occurring on hibernating bats (Courtin et al. 2010; Vanderwolf et al. 2013b). However, in previous studies there was no indication that these *Trichophyton* spp. were represented by anything other than transitory conidia on bats. The concordance of microscopic, culture, molecular, and histopathologic evidence in this study suggests that *T. redellii* is indeed capable of colonizing the skin of presumably healthy hibernating bats.

Although *T. redellii* has not been previously described, it likely is native to North America. Introduced fungal pathogens, like most exotic species, tend to exhibit very low genetic variation as a result of founder effect (e.g., Engelbrecht et al. 2004; Dlugosch and Parker 2008). The genetic diversity in ITS, IGS, and *MCM7* loci of *T. redellii* is inconsistent with recent introduction. In contrast, there has been no observed genetic variation among North American isolates of the bat pathogen *P. destructans* (Ren et al. 2012), a species strongly suspected to have been introduced to North America (Puechmaille et al. 2011). Infections caused by *T. redellii* were, instead, more likely overlooked before the discovery of WNS. The threat of WNS prompted a

heightened awareness of fungal infections, and many state agencies (including WDNR) more intensively monitored hibernating bat populations after the emergence of WNS. Thus, recent discovery of *T. redellii* likely stemmed from increased surveillance.

Bats infected by *T. redellii* exhibit clinical signs that may be confused with WNS (Fig. 1A, B). Specifically, white fungal growth is often evident on exposed skin. Bats with subtle signs generally have visible infections limited to the elbows and wrists, whereas animals with more extensive colonization exhibit white on the forearms and, to a lesser extent, on the wing membranes, hind legs, uropatagium, tail, and ears. In contrast to WNS, clinical manifestation of *T. redellii* infection on the muzzle is apparently rare. With infections of *T. redellii*, the fungal colonization pattern often has an active edge with a central zone of clearing (Fig. 1A), similar to what is observed in classic human ringworm infection (which can be caused by other species of *Trichophyton*; Weitzman and Summerbell 1995). While the "ring" presentation is not typical of WNS, it is also not consistently observed with *T. redellii*; likewise, bats with WNS may lack visible fungus on the muzzle. Thus, field signs alone cannot reliably distinguish the two infections. However, the two conditions can be differentiated by performing a fungal tape impression of the white material and examining fungal morphology under a microscope. While *P. destructans* has distinctive asymmetrically curved, or crescent-shaped conidia borne at the ends of verticillately branched conidiophores (Gargas et al. 2009), *T. redellii* has radially symmetric obovate to pyriform microconidia that attach laterally to the sides or ends of hyphae and are sessile or on very short pedicels (Fig. 1C, D). *Trichophyton redellii* does not form cuplike aggregates of fungal hyphae or cause skin erosion and ulceration characteristic of WNS (Meteyer et al. 2009); rather, *T. redellii* rarely penetrates beyond the epidermis (Fig. 1E, F). Furthermore, bats with *T. redellii* infections have not been observed to exhibit any of the unusual behaviors noted among bats with WNS, such as congregation near the entrances of and premature egression from hibernacula (Turner and Reeder 2009). Infections caused by *T. redellii* were not observed to produce an orange fluorescence when exposed to ultraviolet light (data not shown) as has been reported for *P. destructans* infections (Turner et al. 2014). However, a larger sample size is required to determine whether this technique is reliable for distinguishing between the two infections.

Although *P. destructans* and *T. redellii* are distantly related, the fungi share several key characteristics. Both are slow-growing and psychrophilic, apparently capable of infecting bats only during hibernation when the host's body temperature is greatly reduced. Both may also have soil origins. The genus *Pseudogymnoascus* is well-represented in the sediment of bat hibernacula, and *P. destructans* likely evolved from a soil-dwelling ancestor (Lorch et al. 2013). The closest relatives to *T. redellii* have been found in soil, suggesting that the fungus may be derived from nonpathogenic soil-affiliated species rather than existing pathogenic species that infect other mammalian hosts. Thus, *T. redellii* (along with *P. destructans*) may offer important insight into the factors that drive the evolution of fungal pathogens. Additionally, *T. redellii* could prove to be a valuable model for understanding the epidemiology of WNS because of its biologic and ecologic similarities to *P. destructans*. For example, both fungi may share common transmission routes, adaptations for surviving when their hosts are metabolically active (nonhibernal), and mechanisms that allow colonization of bat skin.

In all sites where *T. redellii* has been found in Wisconsin, no mortality events have been observed and bat populations have either increased or remained rela-

tively stable in the 3 yr that sites have been monitored by WDNR. Thus, it does not appear that *T. redellii* poses a significant threat to populations of native bats. Although the abilities of both *P. destructans* and *T. redellii* to act as infectious agents could be related to a common trait of the host, such as hibernation, the two infections clearly have different outcomes. Future investigation of the relationship between hibernating bats and *T. redellii* may uncover mechanisms by which bats cope with fungal infections during periods of metabolic depression and further explain why *P. destructans* is so deadly.

Infectious diseases in wildlife often shed light on how little we know about host species, pathogens, and the influence of environmental factors on pathogenicity. In the case of WNS, deaths of millions of bats exposed our lack of understanding of interactions between hibernating bats and fungi that share a common environment. We have demonstrated that fungal skin infections are not a novel occurrence among hibernating bats of North America but were likely overlooked before the arrival of *P. destructans* to the continent. Investigating other fungi such as *T. redellii* and the infections they cause could provide an important means by which to study WNS pathogenesis, host and pathogen ecology, and pathogen evolution, in addition to better informing WNS surveillance and diagnostic efforts.

LITERATURE CITED

Anderson JB, Stasovski E. 1992. Molecular phylogeny of northern hemisphere species of *Armillaria*. *Mycologia* 84:505–516.

Blehert DS, Hicks AC, Behr M, Meteyer CU, Berlowski-Zier BM, Buckles EL, Coleman JTH, Darling SR, Gargas A, Niver R, et al. 2009. Bat white-nose syndrome: An emerging fungal pathogen? *Science* 323:227.

Brasch J, Gräser Y. 2005. *Trichophyton eboreum* sp. nov. isolated from human skin. *J Clin Microbiol* 43:5230–5237.

Courtin F, Stone WB, Risatti G, Gilbert K, Van Kruiningen JV. 2010. Pathologic findings and liver elements in hibernating bats with white-nose syndrome. *Vet Pathol* 47:214–219.

Dawson CO, Gentles JC. 1961. The perfect states of *Keratinomyces ajelloi* Vanbreuseghem, *Trichophyton terrestre* Durie & Frey and *Microsporum nanum* Fuentes. *Sabouraudia* 1:49–57.

Dlugosch KM, Parker IM. 2008. Founding events in species invasions: Genetic variation, adaptive evolution, and the role of multiple introductions. *Mol Ecol* 17:431–449.

Durie EB, Frey D. 1957. A new species of *Trichophyton* from New South Wales. *Mycologia* 49:401–411.

Engelbrecht CJ, Harrington TC, Steimel J, Capretti P. 2004. Genetic variation in eastern North America and putatively introduced populations of *Ceratocystis fimbriata* f. *platani*. *Mol Ecol* 13:2995–3005.

Felsenstein J. 1985. Confidence limits on phylogenies: An approach using the bootstrap. *Evolution* 39:783–791.

Gardes M, Bruns TD. 1993. ITS primers with enhanced specificity for basidiomycetes—Application to the identification of mycorrhizae and rusts. *Mol Ecol* 2:113–118.

Gargas A, Trest MT, Christensen M, Volk TJ, Blehert DS. 2009. *Geomyces destructans* sp. nov. associated with bat white-nose syndrome. *Mycotaxon* 108:147–154.

Gräser Y, de Hoog GS, Kuijpers AFA. 2000. Recent advances in the molecular taxonomy of dermatophytes. In: *Biology of dermatophytes and other keratinophilic fungi*, Kushwaha RKS, Guarro J, editors. Revista Iberoamericana de Micología, Bilbao, Spain, pp. 17–21.

Johnson LJAN, Miller AN, McCleery RA, McClanahan R, Kath JA, Lueschow S, Porras-Alfaro A. 2013. Psychrophilic and pyschrotolerant fungi on

bats: *Geomyces* a common fungus on bat wings prior to the arrival of white nose syndrome. *Appl Environ Microbiol* 79:5465–5471.

Katoh K, Standley DM. 2013. MAFFT multiple sequence alignment software version 7: Improvements in performance and usability. *Mol Biol Evol* 30:772–780.

Kornerup A, Wanscher JH. 1978. *Methuen handbook of color*. Eyre Methuen, London, UK, 252 pp.

Largent DL, Johnson D, Watling R. 1977. *How to identify mushrooms to genus III: Microscopic features*. Mad River Press, Eureka, California, 148 pp.

Lorch JM, Gargas A, Meteyer CU, Berlowski-Zier BM, Green DE, Shearn-Bochsler V, Thomas NJ, Blehert DS. 2010. Rapid polymerase chain reaction diagnosis of white-nose syndrome in bats. *J Vet Diagn Invest* 22:224–230.

Lorch JM, Meteyer CU, Behr MJ, Boyles JG, Cryan PM, Hicks AC, Ballmann AE, Coleman JTH, Redell DN, Reeder DM, et al. 2011. Experimental infection of bats with *Geomyces destructans* causes white-nose syndrome. *Nature* 480: 376–378.

Lorch JM, Lindner DL, Gargas A, Muller LK, Minnis AM, Blehert DS. 2013. A culture-based survey of fungi in soil from bat hibernacula in the eastern United States and its implications for detection of *Geomyces destructans*, the causal agent of bat white-nose syndrome. *Mycologia* 105:237–252.

Mantovani A, Morganti L, Battelli G, Mantovani A, Poglayen G, Tampieri MP, Vecchi G. 1982. The role of wild animals in the ecology of dermatophytes and related fungi. *Folia Parasitol (Praha)* 29:279–284.

Meteyer CU, Buckles EL, Blehert DS, Hicks AL, Green DE, Shearn-Bochsler V, Thomas NJ, Gargas A, Behr MJ. 2009. Histopathologic criteria to confirm white-nose syndrome in bats. *J Vet Diagn Invest* 21:411–414.

Miller MA, Pfeiffer W, Schwartz T. 2010. Creating the CIPRES Science Gateway for inference of large phylogenetic trees. In: *Proceedings of the Gateway Computing Environments Workshop (CGE)*, New Orleans, Louisiana, 14 November, pp. 1–8. http://www.phylo.org/sub_sections/portal/sc2010_paper.pdf. Accessed April 2014.

Minnis AM, Lindner DL. 2013. Phylogenetic evaluation of *Geomyces* and allies reveals no close relatives of *Pseudogymnoascus destructans*, comb. nov., in bat hibernacula of eastern North America. *Fungal Biol* 117:638–649.

Muller LK, Lorch JM, Lindner DL, O'Connor M, Gargas A, Blehert DS. 2013. Bat white-nose syndrome: A real-time TaqMan polymerase chain reaction test targeting the intergenic spacer region of *Geomyces destructans*. *Mycologia* 105:253–259.

Puechmaille SJ, Frick WF, Kunz TH, Racey PA, Voigt CC, Wibbelt G, Teeling EC. 2011. White-nose syndrome: Is this emerging disease a threat to European bats? *Trends Ecol Evol* 26:570–576.

Ren P, Haman KH, Last LA, Rajkumar SS, Keel MK, Chaturvedi V. 2012. Clonal spread of *Geomyces destructans* among bats, Midwestern and Southern United States. *Emerg Infect Dis* 18:883–885.

Stamatakis A. 2006. RAxML-VI-HPC: Maximum likelihood–based phylogenetic analyses with thousands of taxa and mixed models. *Bioinformatics* 22:2688–2690.

Stamatakis A, Hoover P, Rougemount J. 2008. A fast bootstrapping algorithm for the RAxML web-servers. *Syst Biol* 57:758–771.

Swofford DL. 2003. *PAUP*. Phylogenetic Analysis Using Parsimony (* and other methods), Version 4*. Sinauer Associates, Sunderland, Massachusetts, http://www.sinauer.com/paup-phylogenetic-analysis-using-parsimony-and-other-methods-4-0-beta.html. Accessed October 2014.

Turner GG, Reeder DM. 2009. Update of white-nose syndrome in bats, September 2009. *Bat Res News* 50:47–53.

Turner GG, Meteyer CU, Barton H, Gumbs JF, Reeder DM, Overton B, Bandouchova H, Bartonička T, Martínková N, Pikula J, et al. 2014. Non-lethal screening of bat-wing skin with the use of UV fluorescence to detect lesions indicative of white-nose syndrome. *J Wildl Dis* 50:566–573.

US Fish and Wildlife Service. 2014. *White-nose syndrome map*. USFWS, Hadley, Massachusetts, whitenosesyndrome.org/resources/map. Accessed October 2014.

Vanderwolf KJ, Malloch D, McAlpine DF, Forbes GJ. 2013a. A world review of fungi, yeasts, and slime molds in caves. *Int J Speleol* 42:77–96.

Vanderwolf KJ, McAlpine DF, Malloch D, Forbes GJ. 2013b. Ectomycota associated with hibernating bats in eastern Canadian caves prior to the emergence of white-nose syndrome. *Northeast Nat* 20:115–130.

Weitzman I, Summerbell RC. 1995. The dermatophytes. *Clin Microbiol Rev* 8:240–259.

White TJ, Bruns T, Lee S, Taylor J. 1990. Amplification and direct sequencing of fungal ribosomal RNA genes for phylogenetics. In: *PCR protocols: A guide to methods and applications*, Innis MA, Gelfand DH, Sninsky JJ, White TJ, editors. Academic Press, New York, New York, pp. 315–322.